

Original Research

Comparative Proteomic Analysis of Irradiation-Induced Radioresistant Breast Cancer Cells Using Label-Free Quantitation

Yingxia Ying^{1,†}, Lei Bian^{1,2,†}, Yiling Meng^{1,†}, Meichao Zhang¹, Yuan Yao^{1,*}, Fang Bo^{3,*}, Dong Li^{1,*}¹Department of Radiation Oncology, Shanghai Ninth People's Hospital, Shanghai Jiaotong University School of Medicine, 200011 Shanghai, China²Department of Breast Oncology, Sun Yat-Sen University Cancer Center, State Key Laboratory of Oncology in South China, Collaborative Innovation Center for Cancer Medicine, 510060 Guangzhou, Guangdong, China³Disinfection Supply Center, Shanghai Ninth People's Hospital, Shanghai Jiaotong University School of Medicine, 200011 Shanghai, China*Correspondence: yaoyuan@shsmu.edu.cn (Yuan Yao); fangbo1201@163.com (Fang Bo); lidong@shsmu.edu.cn (Dong Li)

†These authors contributed equally.

Academic Editor: Milena Georgieva

Submitted: 20 February 2023 Revised: 12 April 2023 Accepted: 29 May 2023 Published: 19 October 2023

Abstract

Background: Breast cancer poses severe threats to human health as radioresistance becomes increasingly prevalent. The mechanisms of radioresistance are hard to expound completely. This study aims to explore proteomic changes of radioresistance, which will help elucidate the potential mechanisms responsible for breast cancer radioresistance and explore potential therapeutic targets. **Methods:** A radioresistant breast cancer cell line was established by repeated irradiation. Liquid Chromatograph Mass Spectrometer (LC-MS) was used to quantify protein expression. Proteomic changes associated with radioresistance were evaluated by proteomic analysis. Further, cell radioresistance and several identified proteins were verified in *in vitro* experiments. **Results:** In the study, more than 3000 proteins were detected, 243 of which were identified as up-regulated proteins and another 633 as down-regulated proteins. Gene Ontology (GO) enrichment analysis indicated that these proteins were mainly expressed in the lysosome and ribosome, associated with coenzyme binding and the structural constituent of the ribosome, involved in mitotic cytokinesis and ribonucleoprotein complex biogenesis. Kyoto Encyclopedia of Genes and Genomes (KEGG) pathway analysis indicated that many biological processes were extensively altered, particularly spliceosome and thermogenesis. It is worth noting that the functions and pathways related to ribosomes were significantly enriched, therefore ribosomal proteins (*RPL6* and *RPS13*) were identified through western blot and highly expressed in relatively radiosensitive cells. Additionally, several identified proteins, including *S100A4*, *RanBP9*, and *ISG15*, were also verified to be differentially expressed in different radiosensitive cells. **Conclusions:** Our results provide a framework for further studies into the mechanisms of radioresistance and serve as a basis to construct a predictive model of radioresistance in breast cancer. Ribosome may participate in the radioresistance of breast cancer, which provides new insights into the proteomic characteristics of the mechanisms of radioresistance.

Keywords: breast cancer; radioresistance; bioinformatics analysis; proteomic analysis; ribosome

1. Introduction

Breast cancer (BC), the most prevalent female cancer accounting for nearly 1/3 of cancers diagnosed in this population [1], is now widely considered as the leading cause of cancer death among females [2]. The BC mortality rate for females of all ages ranges from 0.4 to 3.4/100 per year due to the differences in the degree of economic development and associated social and lifestyle factors [2,3], and continues to decrease year-on-year. This decrease has been attributed to the increased use of screening mammography combined with improved BC treatment [4,5]. Among them, radiotherapy is one of the mainstays in the management of BC, which is either added to mastectomy to eradicate residual subclinical sections or used as a palliative treatment for advanced BC patients without surgical indication [6,7].

Radiotherapy, a type of ionizing radiation, induces DNA damage directly via ionization or indirectly by the generation of reactive oxygen species (ROS), thereby de-

stroying tumor cells [8,9]. Radiation dose and frequency of radiotherapy depend principally on the balance between cure and toxicity of treatment [10]. The recommended dose of radiation for each individual treated by radiotherapy alone is 50–70 Gy in 25 to 35 fractions or equivalent [11–13]. However, a large amount of evidence demonstrated the presence of radioresistance in BC [14–18]. In addition to the inherent radioresistance of cells, an adaptive response of cancer cells to repeated radiation leads to the development of radioresistance, including alterations in the tumor microenvironment [19], signaling [20], and metabolic [21] pathways. Currently, radioresistance has become a major obstacle to successful cancer therapy, accompanied by high mortality (14.5–22.5%) and recurrence rate (2.4–11.5%) [22–24]. The majority of previous studies involving radioresistance in BC focused on ROS-DNA damage. DNA damage promotes DNA damage repair by activating various signal pathways, thus resulting in radioresistance.



Recently, we established a radioresistant BC cell line by repeated ionizing radiation and found that radioresistant BC cells present elevated expression of ataxia-telangiectasia mutated kinase (*ATM*) and increased DNA damage repair efficiency, indicating a potential link between *ATM*, DNA repair pathway, and radioresistance [25]. Additionally, several molecules such as *SERPINE1* (serpin family E member 1) [26], *YB-1* (Y-box binding protein 1) [27,28], *TTK* (TTK protein kinase) [29] and *ARID1A* (AT-rich interaction domain 1A) [30] have also been reported to contribute to radioresistance.

The majority of previous research has focused at the genomics level, which has inevitable limitations and caveats, including RNA degradation, improper transcription, and inability to analyze the post-translation modification and cellular functions [31,32]. As the structural and functional elements of cells, protein is regarded as the ultimate executor and effector of genomic biological information [33]. Qualitative and quantitative analysis of proteins will help to explore the basis and conditions for the realization of cell biological functions. Furthermore, a single protein only provides a limited understanding of the biological pathways [34], and systematic large-scale data analysis is essential for expanding our understanding of pathological mechanisms. Therefore, the concept of proteomics was urgently introduced in 1994 by Marc Wilkins [35]. Proteomics is a complete and independent collection involving biological characteristics and activities, covering all the proteins expressed in the genome [36–38]. Quantitative proteomics provides the difference in protein abundance between healthy samples and tumor samples, as well as relevant information, including protein-protein interactions, signaling pathways, disease prediction, and phenotypic classification [39]. However, due to the limitations of techniques and data analysis methods, the course of proteomics progression in BC seems to be slow and remains in the initial stage [34,40–42], and protein detection coverage ranges from hundreds to thousands [43–45]. Most importantly, it is worth mentioning that previous proteomics studies always adopted the same but imprecise screening criteria for radioresistance-associated proteins, namely the differential proteins between parental cells and radioresistant cells. Thus, it is necessary to conduct a large-scale and systematic study via strict screening criteria to explore the complex radioresistant mechanism.

Herein, using our established radioresistant cells through repeated irradiation [25], and Liquid Chromatograph Mass Spectrometer (LC-MS) to cover more than 3000 proteins, we identified the differential proteins among the radioresistance-related cells lines using a strict triple screening criteria and conducted function and pathway enrichment analysis, thereby facilitating the exploration of radioresistance mechanisms. The identification of novel proteins [46] associated with radioresistance in BC would not only increase our understanding of the molecular mecha-

nisms underlying the therapeutic resistance but also provide tumor molecular characteristics, promote the refinement of BC subtypes, and contribute to the diagnosis, prognosis, and individualized treatment.

2. Methods

2.1 Cell Cultures and the Establishment of Radioresistant Cell Lines

All cell lines were authenticated using the short tandem repeat (STR) technique. Additionally, mycoplasma testing was conducted on the cell lines, and the result was negative. Human BC cell lines (MDA-MB-231) were purchased from ATCC, and human pancreatic cancer cell lines (PANC1 and MIA-PACA2) were obtained from Cell Bank of Type Culture Collection of Chinese Academy of Sciences (Shanghai, China), grown in Dulbecco's Modified Eagle's Medium (DMEM) containing 10% FBS (Gibco, Loughborough, England) and cultured in a 37 °C incubator containing 95% O₂ and 5% CO₂. Cells (1×10^6) were seeded in 10 cm culture disks. Cells were collected and passed into new dishes when the cell density reached approximately 90%.

For the establishment of the radioresistant cell line, as described [25], MDA-MB-231 cells, set to parental BC cell lines, were divided into two groups, PB and PR cells. PR cells were irradiated with 3 Gray (Gy) of X-rays 20 times at a dose rate of 1.43 Gy per minute, with a total dose of 60 Gy over 4 months as radioresistant cell lines [47]. PB cells were treated using the same conditions without irradiation, and used as control cell lines. Compared with PB cells, PR cells had a more stretched and flatter appearance with enhanced anti-apoptotic, migration, and invasion capabilities and presented elevated surviving fraction, reduced percentage of apoptotic cells, and increased DNA damage repair efficiency.

2.2 Study Group and Sample Preparation

PB cells (hereafter named group A) and PR cells (group B) were collected when the cells reached approximately 90% in 10 cm culture disks. Additionally, PB and PR were irradiated with 10 Gy at a dose rate of 1.43 Gy per minute [48,49] and collected after 24 hours (group C and group D, respectively). A total of 3 biological replicates were collected. **Supplementary Fig. 1** shows the grouping details. The cells were washed 3 times with ice-cold phosphate buffer saline (PBS). A total of 1 mL 10M urea was added and incubated for 5 min. Then, the lysates were sonicated for 5 min. After centrifugation (4 °C, 13,000 g × 10 min), the supernatant was determined using a Bradford Protein Quantification Kit. Each sample (60 ug) was added to 5 uL 1 M dithiothreitol (DTT) for 1 h in a 37 °C water bath and then alkylated with 20 uL 1 M iodoacetamide (IAA) for 1h in the dark at room temperature. Then, samples were digested with trypsin (ratio = 50:1) for 14 h at 37 °C. The trypsin activity was stopped by adding 10% of trifluoroacetic

acid. The peptides were desalinated through C18 HPLC columns (Agilent Technologies Inc. Santa Clara, California, USA) before LC–MS/MS analysis.

2.3 LC–MS/MS Analysis

Proteins were quantified using the modified LC–MS/MS (Agilent 1290, Agilent Technologies Inc. Santa Clara, CA, USA; QTRAP 4500, AB Sciex Inc. Foster City, CA, USA) analytical method as described previously [50]. The analysts were blinded to all the information during testing. The C18 column is balanced with 95% solvent A (0.1% formic acid (FA), H₂O). Solvent B was 0.1% FA with 100% acetonitrile (ACN). Samples were eluted from 7% to 100% of solvent B over 75 min with a flow rate of 600 nL/min. After phase liquid chromatography, mass spectrometric data were acquired automatically by Thermo Xcalibur 4.0 software (Thermo Fisher Scientific Inc, Waltham, MA, USA). Samples were run in one technical replicate.

The scanning parameters were set as follows: DDA acquisition mode, TOP20. The resolution of primary MS was 70,000, the maximum injection time was 50 ms, the fragmentation mode was HCD, and the collision energy of 27% was used for fragmentation; the resolution of secondary MS was 18,000, the maximum injection time was 100 ms, the signal threshold was 1e4 ions/s, and the dynamic exclusion time was 30 s.

2.4 Differential Protein Screening Criteria

Up-regulated proteins were defined based on the following conditions: (1) higher expression in group B than that in group A, (2) increased in group D compared with group B, (3) increased in group C compared with group A. Down-regulated proteins were defined based on the following conditions: (1) lower expression in group B than that in group A, (2) decreased in group D compared with group B, (3) declined in group C than that in group A. A schematic is shown in **Supplementary Fig. 2**.

2.5 Clonogenic Survival

Single-cell suspensions were added to 6-well plates in triplicate. After 24 hours, cells were irradiated with 0–6 Gy at a dose rate of 1.43 Gy per minute and then cultured for 14 days. Cell clusters containing over 50 cells were regarded as colonies. The colonies were fixed with 4% paraformaldehyde, stained with crystal violet, and dried naturally. Plating efficiency (PE) = [the mean number of colonies/the number of inoculated cells]. Surviving fraction (SF) was calculated as follows. $SF(d) = \frac{[the\ mean\ PE(d)]}{[the\ mean\ PE(0)]}$, while *d* indicates dGy and 0 means 0Gy. The curve was plotted using the linear-quadratic model in Graph Prism 6.01 (GraphPad Software Inc., San Diego, CA, USA) as described previously [51,52].

2.6 Western Blot

Cells were washed by pre-cooling PBS three times, and proteins were extracted in 100 uL lysis buffer containing protease and phosphatase inhibitor cocktail (MCE, Monmouth Junction, NJ, USA). Then equal amounts of proteins (5 uL) were size-separated in 10% SDS-PAGE gels and transferred to PVDF membranes. Immunoreactive proteins were visualized using ECL following the manufacturer's instructions (Millipore, Boston, MA, USA). The detailed information for primary antibodies used in this study was provided as follows: Rabbit polyclonal antibodies against *SI00A4* (ABClonal, Wuhan, China, #A19109, 1:1000 dilution), *RANBP9* (ABClonal, #A19238, 1:1000 dilution), *ISG15* (ABClonal, #A1182, 1:1000 dilution), *RPL6* (ABClonal, #A15094, 1:1000 dilution), *RPS13* (ABClonal, #A15720, 1:1000 dilution), *β-actin* (Transgene, #HC201, 1:5000 dilution). Secondary antibodies used were goat anti-rabbit IgG-HRP (Cell Signaling Technology, #7074, 1:5000 dilution) and anti-mouse IgG-HRP (Cell Signaling Technology, #7076, 1:5000 dilution). Data were quantified by ImageJ 1.53e (National Institutes of health, Bethesda, MD, USA) and expressed as arbitrary densitometric units relative to *β-actin* expression. All Western blots (WBs) were performed in triplicate.

2.7 Kaplan–Meier Survival Curves

Kaplan–Meier Plotter (<https://www.kmplot.com>) was applied to evaluate the prognosis of BC by selecting the mRNA as a dataset. The relationships between *SI00A4*, *RanBP9*, *ISG15*, *RPL6*, and *RPS13* expression with overall survival (OS) of different time points were analyzed with the hazard ratio (HR) with 95% confidence intervals (CIs) and log-rank *p*-value. “Auto select best cutoff” was set as a method to split patients.

2.8 Data analysis

The LC–MS/MS raw files were searched and quantified by MaxQuant (version 1.6.2.0; Max Planck Institute of Biochemistry, Munich, Bavaria Germany) against UniProt Protein Database (downloaded on 22 April 2021). The enzyme was set by trypsin with up to two missed cleavages; the main research is 4.5 ppm; The fragment mass tolerance is 0.02 Da; The peptide and protein FDR is 0.01; Unique peptides (at least 2 unique peptides) were used for protein quantification. All data were log₂ transformed before analysis. The *t*-test was employed to identify significantly differentially expressed proteins between two independent groups (three biological repeats in each group). According to the $1.5 \cdot |\log_2 \text{fold change (FC)}|$ and $p < 0.05$, the differential proteins were screened. Then the output protein tables were performed for bioinformatics analysis. Venn diagrams were performed using jvenn. Heatmaps were presented using MeV with Pearson correlation. We functionally annotated the differentially expressed proteins by The Gene Ontology (GO) (<https://david.ncifcrf.gov>) and

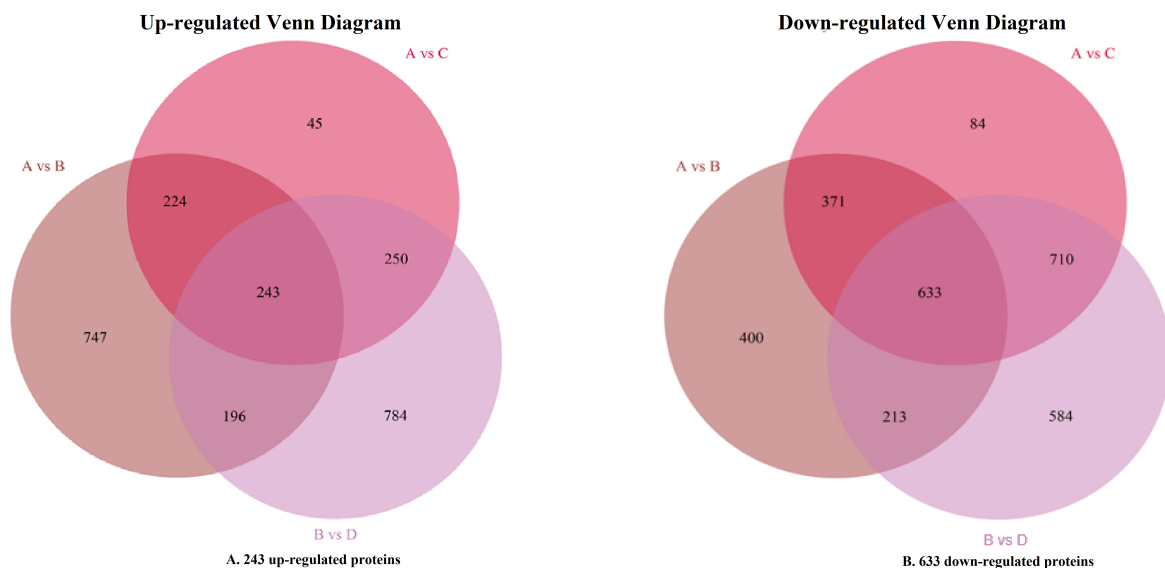


Fig. 1. Protein identification and quantification in three comparison groups. The Venn diagram shows the number of proteins identified in group A vs. C only, group A vs. B only, group B vs. D only, and those shared among three comparison groups. (A) Up-regulated proteins. (B) Down-regulated proteins.

GO-directed acyclic graph to identify associated molecular functions (MF), biological processes (BP), and cellular components (CC). Kyoto Encyclopedia of Genes and Genomes (KEGG) pathway enrichment analysis was generated using KEGG (<http://www.genome.jp/kegg/>) databases to investigate the potential biological interpretation of differentially expressed proteins.

3. Results

3.1 Identification of 876 Significant Proteins by Label Free Quantification (LFQ) Analysis

In this study, quantitative proteomics of radioresistant cells and radiosensitive cells enabled the comparison of protein expression profiles in radiotherapy. Of the 3000+ proteins detected in this study, 876 significant proteins were identified among four groups. From the distribution of the proteins as shown by the Venn diagram, 243 up-regulated proteins were screened (Fig. 1A, **Supplementary Table 1**), and 633 down-regulated differential proteins were found (Fig. 1B, **Supplementary Table 2**) according to the $1.5\text{-}|\log_2 \text{FC}|$ and $p < 0.05$.

3.2 Changes in Identified Proteins Levels in Four Analyzed Groups Using a Heat Map

Although the general relationships of proteins from four groups were visualized using the Venn diagram, it was necessary to consider differences at the concentration level graphically. Heat map analyses, constructed from LFQ intensities, gave a significant overall picture of the up-and down-regulated proteins in each of the samples. The rows (identified proteins) were rearranged according to similar profiles. The columns (samples) are sorted by sample type,

and each sample type in the data matrix is displayed as a color (purple, green, pink, and blue). As shown in Fig. 2, according to the color distribution of the heat map, it can be inferred that the greatest difference in protein expression was between group D and group A. The difference may be attributed to radiotherapy dose and frequency, namely the presence of radioresistance and radiosensitivity.

3.3 GO-Based Annotation and Functional Enrichment Analysis

To evaluate the biological and functional associations of up-and down-regulated proteins, we annotated these proteins based on the GO databases. As shown in Fig. 3A, 243 up-regulated proteins were classified by the second level (biological process, cellular component, and molecular function). Biological process analysis showed these significant proteins participate in RNA splicing and mitotic cytokinesis. Cellular component GO terms significantly enriched in the up-regulated proteins were azurophil granule and primary lysosome. The molecule function is cadherin binding and coenzyme binding. Additionally, down-regulated proteins were enriched in the ribosome and mitochondrial matrix, involved in the ribonucleoprotein complex biogenesis and ribosome biogenesis, also associated with a structural constituent of ribosome and translation initiation factor activity (Fig. 3B). Interestingly, GO analysis of down-regulated proteins has revealed a highly significant correlation with the ribosome, including ribosomal subunit, organellar ribosome, ribosome biogenesis, and other ribosomal processes. It has been conceivably supposed that ribosome may be significant in the pathogenesis of radioresistance.

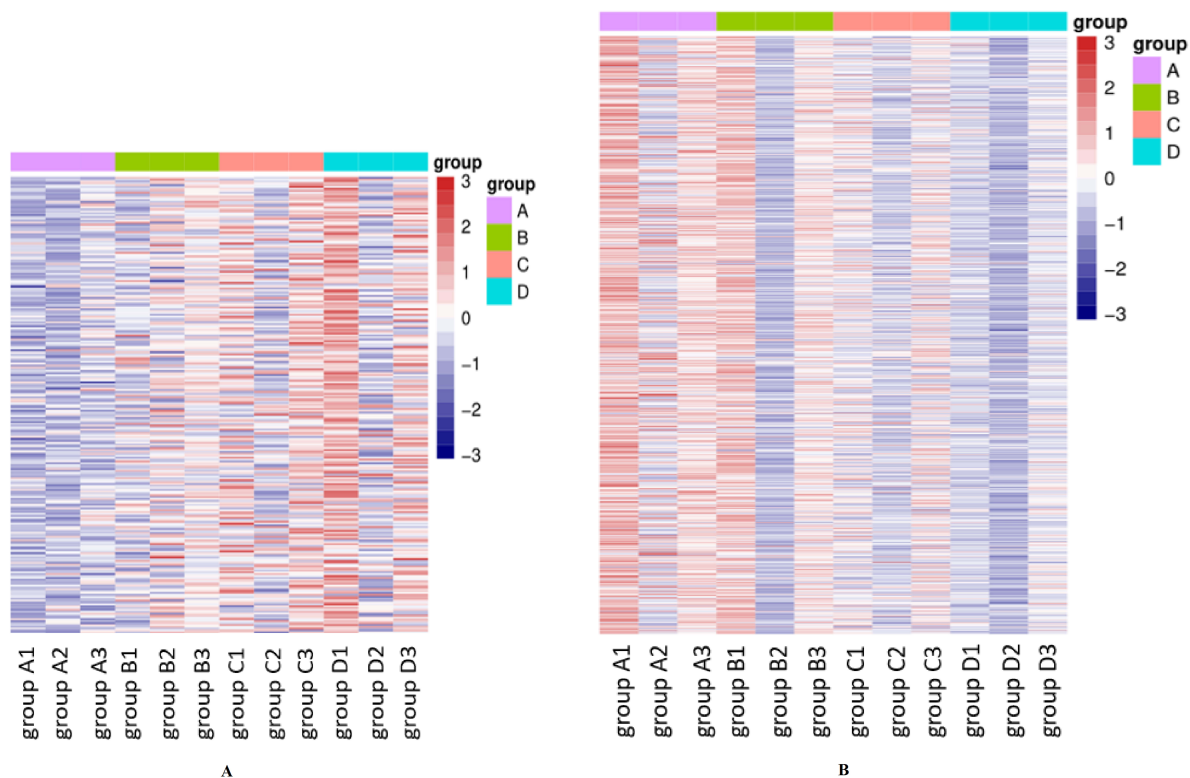


Fig. 2. Heatmap visualization of the significantly different proteins among four groups. Columns: samples; Rows: differential proteins. Color key indicates protein expression value: blue, lowest; red, highest. (A) Up-regulated proteins. (B) Down-regulated proteins.

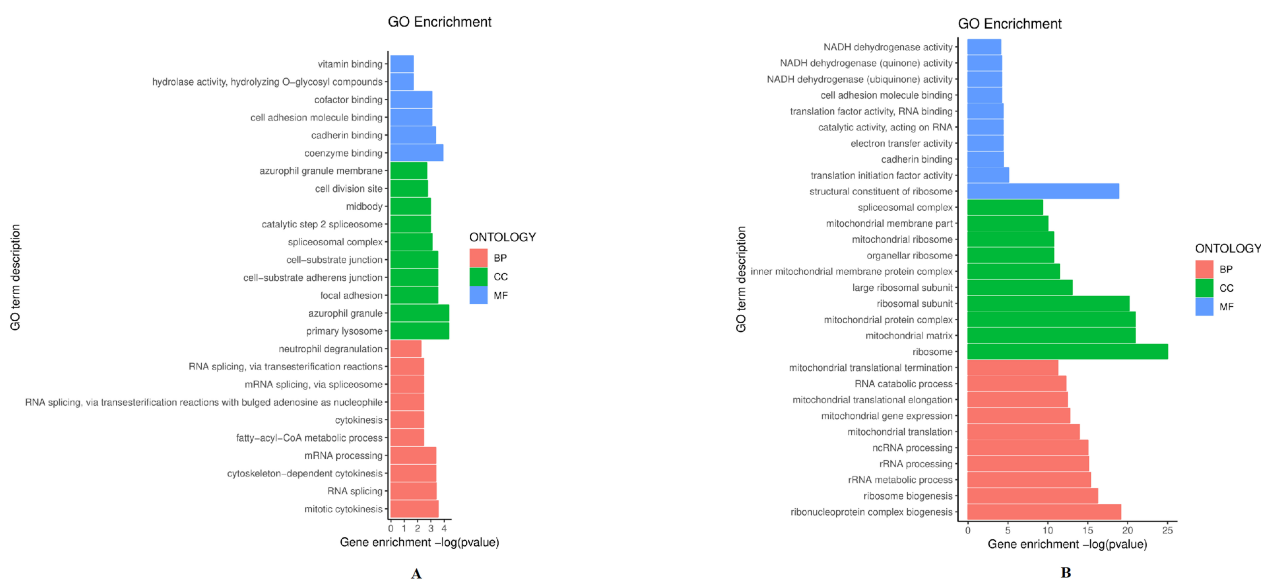


Fig. 3. Gene ontology (GO) classifications of up-regulated proteins (A) and down-regulated proteins (B). The figure shows the top 10 GO terms. Horizontal coordinate: GO enrichment value; vertical coordinate: GO term. BP, biological process; CC, cellular component; MF, molecular function.

Despite the advances in GO annotations, it is necessary to further annotate proteins more comprehensively and precisely. Thus, the directed acyclic graph (DAG) showed

the hierarchical relationship of significantly enriched GO terms, including up- and down-regulated proteins, where hierarchy was defined with respect to the available terms

associated with the proteins. As DAG is shown in Fig. 4, from top to bottom, there were two main paths of GO terms in up-regulated proteins (the number of GO items ≥ 3), including “Path 1: cell-substrate junction (GO:0030055)-cell-substrate adherens junction (GO:0005924)-focal adhesion (GO:0005925)” and “Path 2: primary lysosome (GO:0005766)-azurophil granule (GO:0042582)-azurophil granule membrane (GO:0035577)”. Path 1 and 2 primarily showed the cell adhesion function and lysosomal function, respectively, which have been reported to be related to therapeutic resistance [53,54]. Two main paths of GO terms in down-regulated proteins are shown in Fig. 5, namely “Path 1: ribosome (GO:0005840)-ribosomal subunit (GO:0044391)-large ribosomal subunit (GO:0015934)” and “Path 2: ribosome (GO:0005840)-organellar ribosome (GO:0000313)-mitochondrial ribosome (GO:0005761)”, both focused on ribosomes, suggesting the possibly vital function of ribosomes in radiosensitivity. The related GO terms are listed in **Supplementary Table 3**.

As illustrated, the azurophil granule membrane (GO:0035577) and inner mitochondrial membrane protein complex (GO: 0098800) were the targets of action of up-regulated proteins and down-regulated proteins, respectively. Similar to GO annotations, ribosome (GO: 0005840) and mitochondrial ribosome (GO: 0005761) were up-regulated in the radiosensitivity of BC.

3.4 KEGG Pathway Analysis

To further evaluate the biological significance and investigate the disturbed signaling pathways of these proteins, the association network of differentially expressed proteins was constructed. As depicted in Fig. 6A, the most significantly enriched KEGG pathway in up-regulated proteins was the spliceosome. In addition, thermogenesis was the most important metabolic pathway related to down-regulated proteins (Fig. 6B). In the pathway analysis, several significant pathways were highly enriched, including spliceosome, thermogenesis, Parkinson’s disease, and oxidative phosphorylation. Among these pathways, spliceosome [55] and oxidative phosphorylation [56,57] have been reported to be linked to radioresistance. It is noteworthy that ribosome was strongly enriched among differentially expressed proteins, consistent with GO annotations, further confirming the importance of ribosome for irradiation-induced radiosensitivity/radioresistance.

3.5 Cell Radioresistance and Candidate Proteins Validation

The radioresistance of PB cells and PR cells was compared by surviving fraction (SF). As shown in Fig. 7A, the PR cell line had a higher survival rate than that of PB cells. Next, we randomly selected candidate proteins for validation. *S100A4* (S100 calcium-binding protein A4), *RanBP9* (RAN binding protein 9), *ISG15* (Interferon-induced gene

15), *RPL6* (ribosomal protein L6), and *RPS13* (ribosomal protein S13), which were found differentially expressed in our study, were verified with immunoblotting. Results of western blotting (Fig. 7B) showed that *RanBP9*, *RPL6*, and *RPS13* in PR cells were lower than that of PB cells, while *S100A4* and *ISG15* in PR cells were higher than that in PB cells. What is noteworthy is that *RPL6* [58,59] and *RPS13* [60,61] have been reported to influence multidrug sensitivity in gastric cancer cells, similar to our finding that ribosomal proteins affect radiosensitivity in BC cells.

Next, the impact of *S100A4*, *RanBP9*, *ISG15*, *RPL6*, and *RPS13* expression on prognosis in BC patients was evaluated (**Supplementary Fig. 3**). BC patients with higher *ISG15* or lower *RPS13* expression had significantly shorter overall survival than those with lower *ISG15* or higher *RPS13* expression ($p < 0.05$), respectively, which was consistent with the higher expression of *ISG15* or lower *RPS13* in more malignant and radioresistant cells (Fig. 7B). By contrast, there was no significant difference between the groups with high or low expression of *S100A4*, *RanBP9*, or *RPL6*, which may be due to differences in survival time division, different cut-off time, or other undefined factors.

Further, in order to verify the universality of our findings, we tested the correlation between the expression of *ISG15* and the radioresistance in human pancreatic cancer cell lines (PANC1 and PACA2) (**Supplementary Fig. 4**). Similar to the results of PR and PB cells, the expression of *ISG15* in PACA2 cells is higher than that in PANC1, whereas the SF of PACA2 is higher than that of PANC1 (**Supplementary Fig. 2**).

4. Discussion

Here, we performed a label-free quantitative proteomics analysis of radiosensitive and radioresistant cells to investigate radioresistance-related proteins.

Among 876 differentially expressed proteins, some proteins have been reported to be related to drug resistance in previous studies, such as *S100A4* [62–64], *RanBP9* [65,66] and *ISG15* [67,68], which are consistent with WB verification in our study. Other differentially expressed proteins, such as *LARP4B*, *CAPRINI*, and *PLOD3*, need further expression and functional confirmation. In the future, clinically relevant models can be constructed based on these identified proteins to forecast the radioresistance of patients as a precision medicine tool.

In our study, both enrichment analysis and WB results indicated a possible role of ribosomes in the development of radioresistance. Indeed, evidence has emerged in recent decades regarding the close link between ribosome and therapeutic resistance in cancers.

Ribosome is a complex of ribosomal RNA (rRNA) and ribosomal proteins [69], which synthesize proteins in living cells. Ribosome biogenesis and processing are under surveillance of multiple checkpoints and pathways [70]. As an essential component of the 50S subunit of ribosomes,

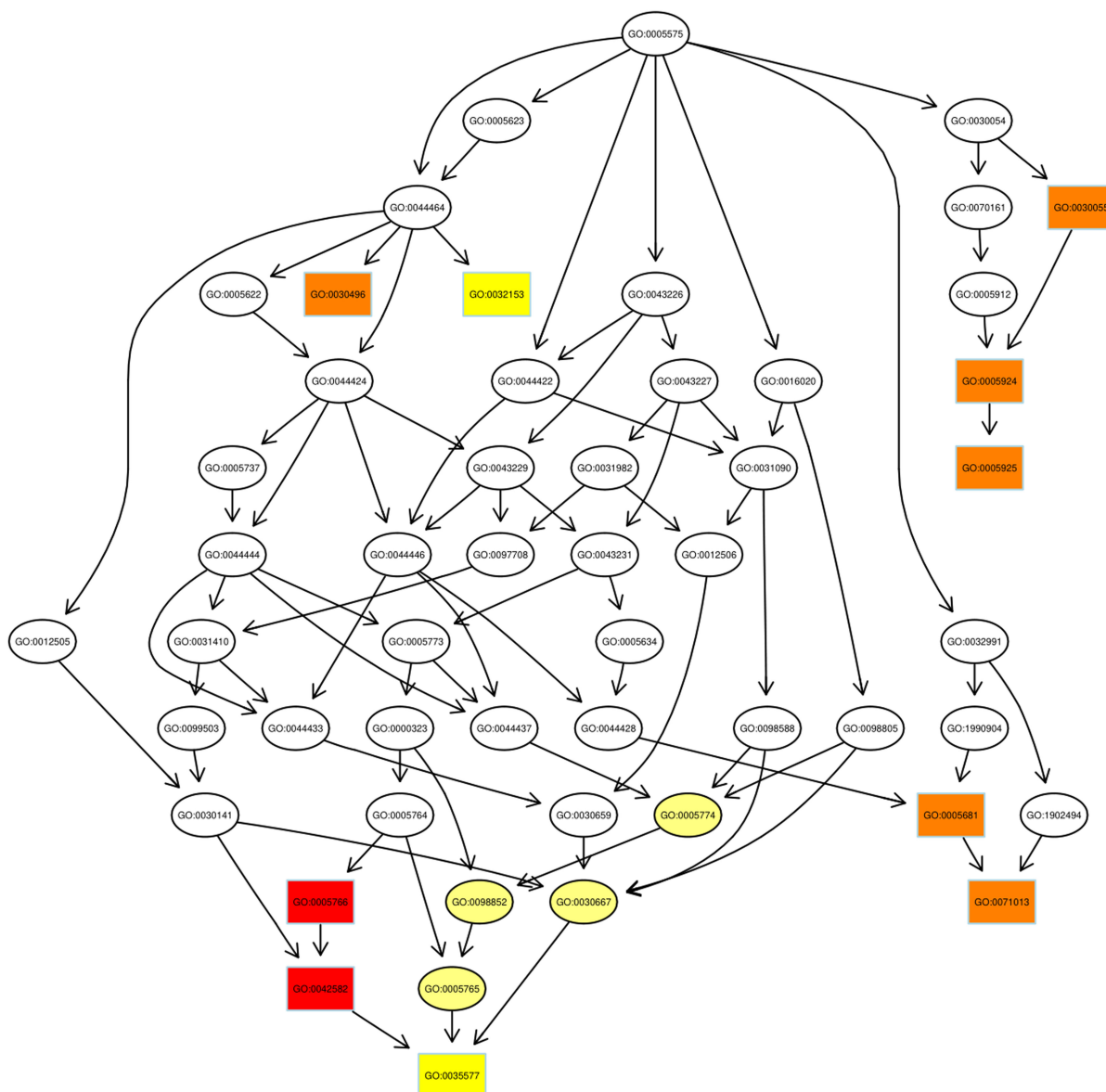


Fig. 4. Pathway analysis of up-regulated proteins using directed acyclic graph (DAG). Boxes were used to indicate the top 10 terms with high salience, and the figure shows the corresponding relationship of each layer. Different colors represent different enrichment salience: the redder color, the higher salience.

RPL6 is a highly conserved ribosome protein [71]. Previous studies have shown that *RPL6* can up-regulate *Bcl-2* and down-regulate *Bax* [59,72]; Inhibition of *RPL6* inhibits the transition from G1 to S phase [58,73,74]; Decreased *RPL6* can reduce ubiquitin-dependent peptide presentation and trigger tumor immune escape [75]. Moreover, it has been suggested that *RPL6* can be recruited to DNA damage sites and regulate DNA damage response in a poly (ADP-ribose) polymerase-dependent manner [76,77]. Evidently, *RPL6* can inhibit tumor cell apoptosis and increase therapy resistance through the above mechanisms.

RPS13 is a common and stable protein [78], which is primarily distributed in the cytoplasm and associated with

rRNA in the large and small subunits of the ribosome. The knock down of *RPS13* led to G1 arrest [60]; *RPS13* increased the expression level of *Bcl-2* and *Bcl-2/Bax* ratio and induced drug resistance of gastric cancer cells to a certain extent [61].

Under radiation stimulation, DNA is damaged and then activates the DNA damage reaction (DDR) [79]. According to the extent of damage, DDR will develop in the direction of repairing DNA damage to maintain cell survival or activating programmed cell death pathways to accelerate cell death [80]. Among them, the high efficiency of DNA damage repair repairs radiation-induced DNA damage, leading to resistance to apoptosis [81], which is the

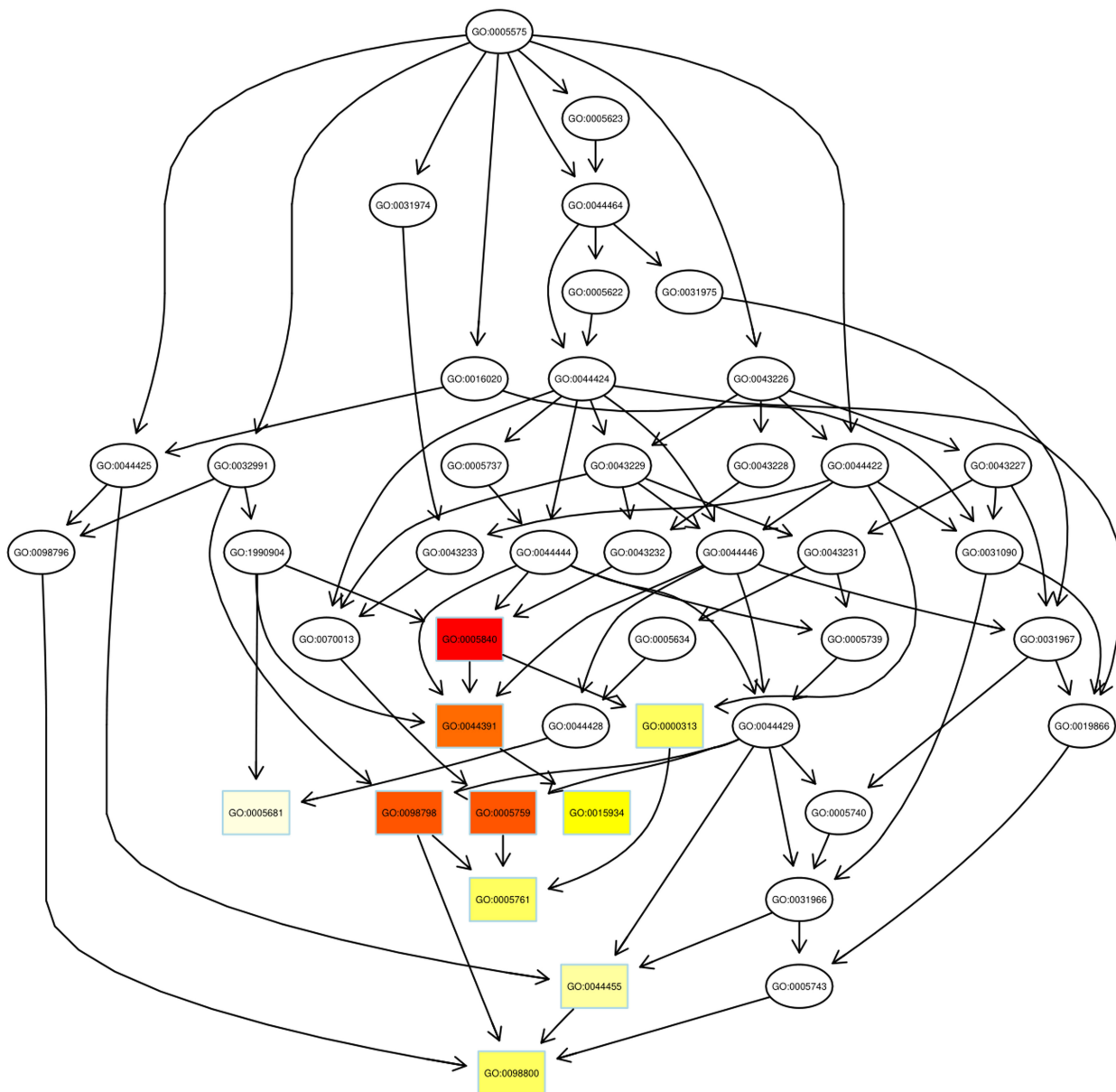


Fig. 5. Pathway analysis of down-regulated proteins using DAG. Boxes were used to indicate the top 10 terms with high salience, and the figure shows the corresponding relationship of each layer. Different colors represent different enrichment salience: the redder color, the higher salience.

main cause of radioresistance [82]; in the process, ribosomal proteins (such as *RPL6* and *RPS13*) play an important role in the regulation of cell cycle and apoptosis (mentioned above), thus affecting the repair efficiency. Apart from ribosomal proteins, associated ribosome biogenesis factors, such as *Bop1* [83], could increase cell recovery by DNA repair regulation, whereas nucleolin [84] played the opposite role.

Most studies involving ribosomes focus on the correlation between gastrointestinal cancer and drug resistance, and there are very few studies involving radioresistance and BC [14,85]. In our study, radioresistance-related proteins

were screened completely and systematically by proteomic analysis, and the findings emphasized the crucial role of ribosomes in radioresistance. Therefore, follow-up research could focus on the association between ribosome and radioresistance, aiming at providing new therapeutic targets for BC.

In addition to ribosomes, KEGG pathway enrichment showed that spliceosome, thermogenesis, and oxidative phosphorylation have a potential correlation with radioresistance. Previous studies have reported that genes involved in spliceosome assembly were significantly up-regulated in BC [86]. Scholars speculated that the spliceosome may

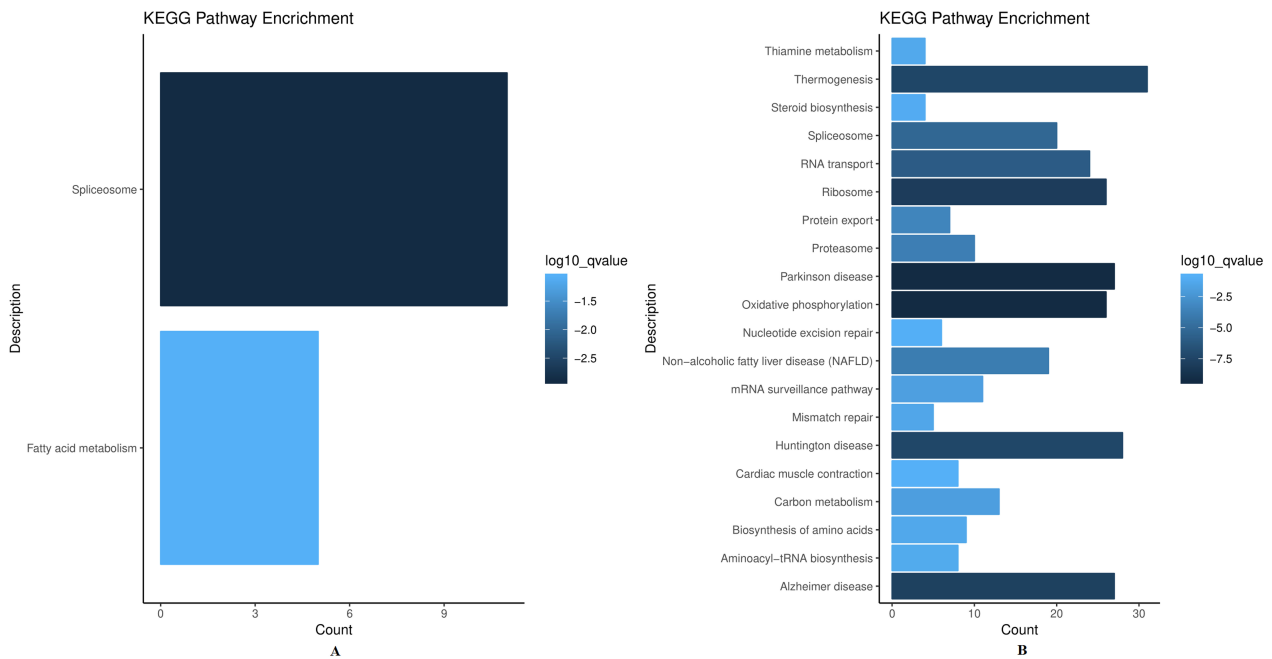


Fig. 6. Significantly enriched pathways from Kyoto Encyclopedia of Genes and Genomes (KEGG). The figure shows the top 20 KEGG pathways ($p < 0.05$). The color of the bar indicates the number of proteins detected for that pathway and the adjusted p -value, respectively. (A) Up-regulated proteins. (B) Down-regulated proteins.

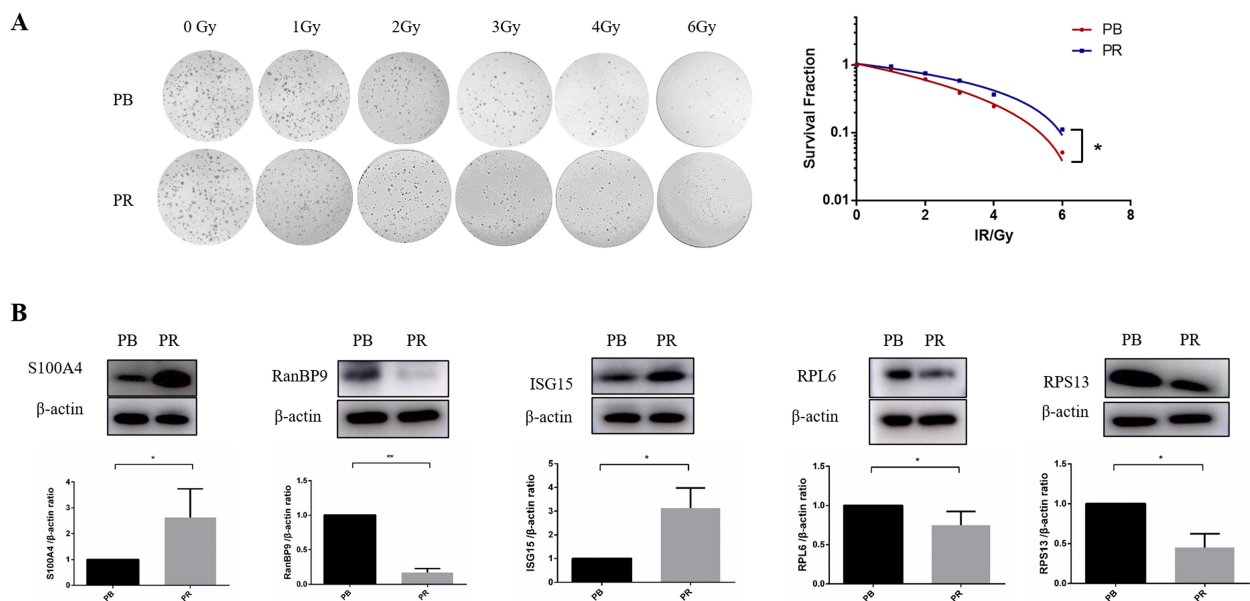


Fig. 7. Surviving fraction in PB and PR cells and validation of differential proteins. (A) Surviving fraction of PB and PR cells. Representative images (left panel) and the quantitative analysis of three independent experiments (right panel) are shown, respectively. (B) Western blot of *S100A4*, *RanBP9*, *ISG15*, *RPL6*, and *RPS13* in PB and PR cells. β -actin was a loading control. A typical experiment of three independent experiments is shown (top panel). Relative protein levels of *S100A4*, *RanBP9*, *ISG15*, *RPL6*, and *RPS13* in PB and PR cells with four independent treatments (bottom panel). All values were normalized to the level (=1) in PB cells. Each bar represents the mean \pm SD. $**p < 0.01$, $*p < 0.05$. PB: MDA-MB-231-PB; PR: MDA-MB-231-PR.

play an important mediation role in the tumor microenvironment via cell signal transduction and gene expression regulation [87]. Thermogenesis and oxidative phosphory-

lation are highly regarded metabolic pathways. As an important part of the tumor microenvironment, thermogenesis can provide an energy source [88], in turn promoting tumor

progress [89,90]. Oxidative phosphorylation is over-active in many cancers [91] and aggravates the carcinogenic behaviors by the hypoxia pathway [92–94], thereby maintaining drug resistance and resulting in poor prognosis [95,96].

The findings of our study not only provide a reliable theoretical basis for exploring the mechanism of radioresistance but also provide a data set of radiosensitivity-related proteins for building an evaluation model of individual radiosensitivity. Each individual's radiosensitivity is varied and unpredictable [97]. Therefore, it is necessary to establish a model to evaluate the individual's radiosensitivity so as to formulate a more appropriate radiotherapy strategy and obtain the maximum therapeutic benefit with minimal toxicity. In addition, there are already a variety of BC proteins and transcripts as biomarkers. If the differentially expressed protein screened in the study is used as a new biomarker, it must be tested in validation studies with clinical samples in advance.

It is worth mentioning that strict screening criteria were used in the study. Most mass spectrometry analyses only detected the differentially expressed proteins between susceptible and tolerant cell lines and then defined these proteins as sensitivity or resistance-related proteins. However, during the culture process, the cells inevitably produce radiotherapy-independent proteins. Therefore, we included radiation factors (i.e., irradiated groups C and D) to further screen sensitivity or resistance-related proteins.

However, as the biological functions of ribosomes on radiosensitivity remain largely unexplained, future studies are warranted to confirm our findings. Our study was also restricted to BC cell lines. Therefore, caution is needed if generalizing the findings to other cancers and replication research in diverse cancer cells is warranted.

In conclusion, our study screened potential radioresistance-related proteins, which provide a rationale for further investigation of radioresistance and subserve to develop an appropriate predictive model for the evaluation of radioresistance in BC. Moreover, the interaction of ribosomes with radioresistance may serve as a promising therapeutic strategy. However, a detailed delineation of the mechanism of modulating BC radioresistance awaits future experimentation.

5. Conclusions

In conclusion, our study screened potential radioresistance-related proteins, which provide a rationale for further investigation of radioresistance and subserve to develop an appropriate predictive model for the evaluation of radioresistance in BC. Moreover, the interaction of ribosomes with radioresistance may serve as a promising therapeutic strategy. However, a detailed delineation of the mechanism of modulating BC radioresistance awaits future experimentation.

Availability of Data and Materials

The datasets used and/or analyzed during the current study are available from the corresponding author on reasonable request.

Author Contributions

Study design and concept: DL, YXY, LB, YY. Data acquisition: YXY, LB, YLM, MCZ. Data analysis and interpretation: YXY, LB, YLM, MCZ, FB. Manuscript preparation: DL, YXY, YLM, FB, YY. Manuscript review: YXY, DL, FB, YY. All authors contributed to editorial changes in the manuscript. All authors read and approved the final manuscript. All authors have participated sufficiently in the work to take public responsibility for appropriate portions of the content and agreed to be accountable for all aspects of the work in ensuring that questions related to its accuracy or integrity.

Ethics Approval and Consent to Participate

Not applicable.

Acknowledgment

Not applicable.

Funding

This work was supported by the National Natural Science Foundation of China under Grant 81970094; The Program for Professor of Special Appointment (Eastern Scholar) at Shanghai Institutions of Higher Learning under TP2015022; Shanghai Pujiang Program under Grant 15PJ1404800.

Conflict of Interest

The authors declare no conflict of interest.

Supplementary Material

Supplementary material associated with this article can be found, in the online version, at <https://doi.org/10.31083/j.fbl2810244>.

References

- [1] Krisanits B, Randise JF, Burton CE, Findlay VJ, Turner DP. Pubertal mammary development as a “susceptibility window” for breast cancer disparity. *Advances in Cancer Research*. 2020; 146: 57–82.
- [2] Bray F, Ferlay J, Soerjomataram I, Siegel RL, Torre LA, Jemal A. Global cancer statistics 2018: GLOBOCAN estimates of incidence and mortality worldwide for 36 cancers in 185 countries. *CA - A Cancer Journal for Clinicians*. 2018; 68: 394–424.
- [3] Hendrick RE, Baker JA, Helvie MA. Breast cancer deaths averted over 3 decades. *Cancer*. 2019; 125: 1482–1488.
- [4] Tabár L, Dean PB, Chen THH, Yen AMF, Chen SLS, Fann JCY, *et al.* The incidence of fatal breast cancer measures the increased effectiveness of therapy in women participating in mammography screening. *Cancer*. 2019; 125: 515–523.

- [5] Kaplan HG, Malmgren JA, Atwood MK, Calip GS. Effect of treatment and mammography detection on breast cancer survival over time: 1990-2007. *Cancer*. 2015; 121: 2553–2561.
- [6] Bradley JA, Mendenhall NP. Novel Radiotherapy Techniques for Breast Cancer. *Annual Review of Medicine*. 2018; 69: 277–288.
- [7] He MY, Rancoule C, Rehailla-Blanchard A, Espenel S, Trone JC, Bernichon E, *et al.* Radiotherapy in triple-negative breast cancer: Current situation and upcoming strategies. *Critical Reviews in Oncology/Hematology*. 2018; 131: 96–101.
- [8] Lee SY, Jeong EK, Ju MK, Jeon HM, Kim MY, Kim CH, *et al.* Induction of metastasis, cancer stem cell phenotype, and oncogenic metabolism in cancer cells by ionizing radiation. *Molecular Cancer*. 2017; 16: 10.
- [9] Petroni G, Cantley LC, Santambrogio L, Formenti SC, Galluzzi L. Radiotherapy as a tool to elicit clinically actionable signalling pathways in cancer. *Nature Reviews Clinical Oncology*. 2022; 19: 114–131.
- [10] Barnett GC, West CML, Dunning AM, Elliott RM, Coles CE, Pharoah PDP, *et al.* Normal tissue reactions to radiotherapy: towards tailoring treatment dose by genotype. *Nature Reviews Cancer*. 2009; 9: 134–142.
- [11] Recht A, Edge SB, Solin LJ, Robinson DS, Estabrook A, Fine RE, *et al.* Postmastectomy radiotherapy: clinical practice guidelines of the American Society of Clinical Oncology. *Journal of Clinical Oncology*. 2001; 19: 1539–1569.
- [12] Arriagada R, Mouriessse H, Sarrazin D, Clark RM, Deboer G. Radiotherapy alone in breast cancer. I. Analysis of tumor parameters, tumor dose and local control: the experience of the Gustave-Roussy Institute and the Princess Margaret Hospital. *International Journal of Radiation Oncology Biology Physics*. 1985; 11: 1751–1757.
- [13] Van Limbergen E, Van der Schueren E, Van den Bogaert W, Van Wing J. Local control of operable breast cancer after radiotherapy alone. *European Journal of Cancer*. 1990; 26: 674–679.
- [14] Choi J, Yoon YN, Kim N, Park CS, Seol H, Park IC, *et al.* Predicting radiation resistance in breast cancer with expression status of phosphorylated S6K1. *Scientific Reports*. 2020; 10: 641.
- [15] Speers C, Zhao S, Liu M, Bartelink H, Pierce LJ, Feng FY. Development and validation of a novel radiosensitivity signature in human breast cancer. *Clinical Cancer Research*. 2015; 21: 3667–3677.
- [16] Duru N, Fan M, Candas D, Menea C, Liu HC, Nantajit D, *et al.* HER2-associated radioresistance of breast cancer stem cells isolated from HER2-negative breast cancer cells. *Clinical Cancer Research*. 2012; 18: 6634–6647.
- [17] Zhang X, Xie K, Zhou H, Wu Y, Li C, Liu Y, *et al.* Role of non-coding RNAs and RNA modifiers in cancer therapy resistance. *Molecular Cancer*. 2020; 19: 47.
- [18] Candas-Green D, Xie B, Huang J, Fan M, Wang A, Menea C, *et al.* Dual blockade of CD47 and HER2 eliminates radioresistant breast cancer cells. *Nature Communications*. 2020; 11: 4591.
- [19] Suwa T, Kobayashi M, Nam JM, Harada H. Tumor microenvironment and radioresistance. *Experimental and Molecular Medicine*. 2021; 53: 1029–1035.
- [20] Atashzar MR, Baharlou R, Karami J, Abdollahi H, Rezaei R, Pourramezan F, *et al.* Cancer stem cells: A review from origin to therapeutic implications. *Journal of Cellular Physiology*. 2020; 235: 790–803.
- [21] Tang L, Wei F, Wu Y, He Y, Shi L, Xiong F, *et al.* Role of metabolism in cancer cell radioresistance and radiosensitization methods. *Journal of Experimental and Clinical Cancer Research*. 2018; 37: 87.
- [22] Orecchia R, Veronesi U, Maisonneuve P, Galimberti VE, Lazzeri R, Veronesi P, *et al.* Intraoperative irradiation for early breast cancer (ELIOT): long-term recurrence and survival outcomes from a single-centre, randomised, phase 3 equivalence trial. *The Lancet Oncology*. 2021; 22: 597–608.
- [23] Wickberg A, Holmberg L, Adami HO, Magnuson A, Villman K, Liljegren G. Sector resection with or without postoperative radiotherapy for stage I breast cancer: 20-year results of a randomized trial. *Journal of Clinical Oncology*. 2014; 32: 791–797.
- [24] Liljegren G, Holmberg L, Bergh J, Lindgren A, Tabár L, Nordgren H, *et al.* 10-Year results after sector resection with or without postoperative radiotherapy for stage I breast cancer: a randomized trial. *Journal of Clinical Oncology*. 1999; 17: 2326–2333.
- [25] Bian L, Meng Y, Zhang M, Guo Z, Liu F, Zhang W, *et al.* ATM expression is elevated in established radiation-resistant breast cancer cells and improves DNA repair efficiency. *International Journal of Biological Sciences*. 2020; 16: 1096–1106.
- [26] Su YH, Wu YZ, Ann DK, Chen JLY, Kuo CY. Obesity promotes radioresistance through SERPINE1-mediated aggressiveness and DNA repair of triple-negative breast cancer. *Cell Death and Disease*. 2023; 14: 53.
- [27] Lettau K, Khozooei S, Kosnopfel C, Zips D, Schitteck B, Toulany M. Targeting the y-box binding protein-1 axis to overcome radiochemotherapy resistance in solid tumors. *International Journal of Radiation Oncology Biology Physics*. 2021; 111: 1072–1087.
- [28] Khozooei S, Lettau K, Barletta F, Jost T, Rebholz S, Veerapan S, *et al.* Fisetin induces DNA double-strand break and interferes with the repair of radiation-induced damage to radiosensitize triple negative breast cancer cells. *Journal of Experimental and Clinical Cancer Research*. 2022; 41: 256.
- [29] Chandler BC, Moubadder L, Ritter CL, Liu M, Cameron M, Wilder-Romans K, *et al.* TTK inhibition radiosensitizes basal-like breast cancer through impaired homologous recombination. *The Journal of Clinical Investigation*. 2020; 130: 958–973.
- [30] Andrade D, Mehta M, Griffith J, Oh S, Corbin J, Babu A, *et al.* HuR Reduces Radiation-Induced DNA Damage by Enhancing Expression of ARID1A. *Cancers*. 2019; 11: 2014.
- [31] Amerik AY, Hochstrasser M. Mechanism and function of deubiquitinating enzymes. *Biochimica et Biophysica Acta*. 2004; 1695: 189–207.
- [32] Yeh E, Cunningham M, Arnold H, Chasse D, Monteith T, Ivaldi G, *et al.* A signalling pathway controlling c-Myc degradation that impacts oncogenic transformation of human cells. *Nature Cell Biology*. 2004; 6: 308–318.
- [33] Franciosa G, Kverneland AH, Jensen AWP, Donia M, Olsen JV. Proteomics to study cancer immunity and improve treatment. *Seminars in Immunopathology*. 2023; 45: 241–251.
- [34] Chae YK, Gonzalez-Angulo AM. Implications of functional proteomics in breast cancer. *The Oncologist*. 2014; 19: 328–335.
- [35] Wilkins M. Proteomics data mining. *Expert Review of Proteomics*. 2009; 6: 599–603.
- [36] Cheung CHY, Juan HF. Quantitative proteomics in lung cancer. *Journal of Biomedical Science*. 2017; 24: 37.
- [37] Ankney JA, Muneer A, Chen X. Relative and Absolute Quantitation in Mass Spectrometry-Based Proteomics. *Annual Review of Analytical Chemistry*. 2018; 11: 49–77.
- [38] Zhang Z, Wu S, Stenoien DL, Paša-Tolić L. High-throughput proteomics. *Annual Review of Analytical Chemistry*. 2014; 7: 427–454.
- [39] Cifani P, Kentsis A. Towards comprehensive and quantitative proteomics for diagnosis and therapy of human disease. *Proteomics*. 2017; 17: 1600079.
- [40] Johansson HJ, Socciarelli F, Vacanti NM, Haugen MH, Zhu Y, Siavelis I, *et al.* Breast cancer quantitative proteome and proteogenomic landscape. *Nature Communications*. 2019; 10: 1600.

- [41] Smith L, Qutob O, Watson MB, Beavis AW, Potts D, Welham KJ, *et al.* Proteomic identification of putative biomarkers of radiotherapy resistance: a possible role for the 26S proteasome? *Neoplasia*. 2009; 11: 1194–1207.
- [42] Meehan J, Gray M, Martínez-Pérez C, Kay C, Wills JC, Kunkler IH, *et al.* A Novel Approach for the Discovery of Biomarkers of Radiotherapy Response in Breast Cancer. *Journal of Personalized Medicine*. 2021; 11: 796.
- [43] Nie S, McDermott SP, Deol Y, Tan Z, Wicha MS, Lubman DM. A quantitative proteomics analysis of MCF7 breast cancer stem and progenitor cell populations. *Proteomics*. 2015; 15: 3772–3783.
- [44] Chang HY, Li MH, Huang TC, Hsu CL, Tsai SR, Lee SC, *et al.* Quantitative proteomics reveals middle infrared radiation-interfered networks in breast cancer cells. *Journal of Proteome Research*. 2015; 14: 1250–1262.
- [45] Lin Y, Lin L, Fu F, Wang C, Hu A, Xie J, *et al.* Quantitative proteomics reveals stage-specific protein regulation of triple negative breast cancer. *Breast Cancer Research and Treatment*. 2021; 185: 39–52.
- [46] Nicolini A, Ferrari P, Duffy MJ. Prognostic and predictive biomarkers in breast cancer: Past, present and future. *Seminars in Cancer Biology*. 2018; 52: 56–73.
- [47] Fukuda K, Sakakura C, Miyagawa K, Kuriu Y, Kin S, Nakase Y, *et al.* Differential gene expression profiles of radioresistant oesophageal cancer cell lines established by continuous fractionated irradiation. *British Journal of Cancer*. 2014; 91: 1543–1550.
- [48] Ishihara S, Yasuda M, Ishizu A, Ishikawa M, Shirato H, Haga H. Activating transcription factor 5 enhances radioresistance and malignancy in cancer cells. *Oncotarget*. 2015; 6: 4602–4614.
- [49] Li JY, Li YY, Jin W, Yang Q, Shao ZM, Tian XS. ABT-737 reverses the acquired radioresistance of breast cancer cells by targeting Bcl-2 and Bcl-xL. *Journal of Experimental and Clinical Cancer Research*. 2012; 31: 102.
- [50] Kang Y, Liu Z, Shi H, Wang J, Huang J, Li Y, *et al.* Label-free quantification of protein expression in the rainbow trout (*Oncorhynchus mykiss*) in response to short-term exposure to heat stress. *Comparative Biochemistry and Physiology - Part D: Genomics and Proteomics*. 2019; 30: 158–168.
- [51] Morak MJM, van Koetsveld PM, Kanaar R, Hofland LJ, van Eijck CHJ. Type I interferons as radiosensitisers for pancreatic cancer. *European Journal of Cancer*. 2011; 47: 1938–1945.
- [52] Rofstad EK, Ruud EBM, Mathiesen B, Galappathi K. Associations between radiocurability and interstitial fluid pressure in human tumor xenografts without hypoxic tissue. *Clinical Cancer Research*. 2010; 16: 936–945.
- [53] Niu H, Qian L, Luo Y, Wang F, Zheng H, Gao Y, *et al.* Targeting of VPS18 by the lysosomotropic agent RDN reverses TFE3-mediated drug resistance. *Signal Transduction and Targeted Therapy*. 2021; 6: 224.
- [54] Correia AL, Bissell MJ. The tumor microenvironment is a dominant force in multidrug resistance. *Drug Resistance Updates*. 2012; 15: 39–49.
- [55] Tanaka I, Chakraborty A, Saulnier O, Benoit-Pilven C, Vacher S, Labiod D, *et al.* ZRANB2 and SYF2-mediated splicing programs converging on ECT2 are involved in breast cancer cell resistance to doxorubicin. *Nucleic Acids Research*. 2020; 48: 2676–2693.
- [56] Boreel DF, Span PN, Heskamp S, Adema GJ, Bussink J. Targeting Oxidative Phosphorylation to Increase the Efficacy of Radio- and Immune-Combination Therapy. *Clinical Cancer Research*. 2021; 27: 2970–2978.
- [57] Chen D, Barsoumian HB, Fischer G, Yang L, Verma V, Younes AI, *et al.* Combination treatment with radiotherapy and a novel oxidative phosphorylation inhibitor overcomes PD-1 resistance and enhances antitumor immunity. *Journal for Immunotherapy of Cancer*. 2020; 8: e000289.
- [58] Wu Q, Gou Y, Wang Q, Jin H, Cui L, Zhang Y, *et al.* Downregulation of RPL6 by siRNA inhibits proliferation and cell cycle progression of human gastric cancer cell lines. *PLoS ONE*. 2011; 6: e26401.
- [59] Du J, Shi Y, Pan Y, Jin X, Liu C, Liu N, *et al.* Regulation of multidrug resistance by ribosomal protein l6 in gastric cancer cells. *Cancer Biology and Therapy*. 2005; 4: 242–247.
- [60] Guo X, Shi Y, Gou Y, Li J, Han S, Zhang Y, *et al.* Human ribosomal protein S13 promotes gastric cancer growth through down-regulating p27(Kip1). *Journal of Cellular and Molecular Medicine*. 2011; 15: 296–306.
- [61] Shi Y, Zhai H, Wang X, Han Z, Liu C, Lan M, *et al.* Ribosomal proteins S13 and L23 promote multidrug resistance in gastric cancer cells by suppressing drug-induced apoptosis. *Experimental Cell Research*. 2004; 296: 337–346.
- [62] Zhang J, Hou S, Gu J, Tian T, Yuan Q, Jia J, *et al.* S100A4 promotes colon inflammation and colitis-associated colon tumorigenesis. *Oncoimmunology*. 2018; 7: e1461301.
- [63] Prasmickaite L, Tenstad EM, Pettersen S, Jabeen S, Egeland EV, Nord S, *et al.* Basal-like breast cancer engages tumor-supportive macrophages via secreted factors induced by extracellular S100A4. *Molecular Oncology*. 2018; 12: 1540–1558.
- [64] Song Z, Jia G, Ma P, Cang S. Exosomal miR-4443 promotes cisplatin resistance in non-small cell lung carcinoma by regulating FSP1 m6A modification-mediated ferroptosis. *Life Sciences*. 2021; 276: 119399.
- [65] Tessari A, Parbhoo K, Pawlikowski M, Fassan M, Rulli E, Foray C, *et al.* RANBP9 affects cancer cells response to genotoxic stress and its overexpression is associated with worse response to platinum in NSCLC patients. *Oncogene*. 2018; 37: 6463–6476.
- [66] Dai H, Lv YF, Yan GN, Meng G, Zhang X, Guo QN. RanBP9/TSSC3 complex cooperates to suppress anoikis resistance and metastasis via inhibiting Src-mediated Akt signaling in osteosarcoma. *Cell Death and Disease*. 2016; 7: e2572.
- [67] Huo Y, Zong Z, Wang Q, Zhang Z, Deng H. ISG15 silencing increases cisplatin resistance via activating p53-mediated cell DNA repair. *Oncotarget*. 2017; 8: 107452–107461.
- [68] Yan S, Kumari M, Xiao H, Jacobs C, Kochumon S, Jedrychowski M, *et al.* IRF3 reduces adipose thermogenesis via ISG15-mediated reprogramming of glycolysis. *The Journal of Clinical Investigation*. 2021; 131: e144888.
- [69] Baßler J, Hurt E. Eukaryotic Ribosome Assembly. *Annual Review of Biochemistry*. 2019; 88: 281–306.
- [70] Moudry P, Chroma K, Bursac S, Volarevic S, Bartek J. RNA-interference screen for p53 regulators unveils a role of WDR75 in ribosome biogenesis. *Cell Death and Differentiation*. 2022; 29: 687–696.
- [71] Shigeno Y, Uchiumi T, Nomura T. Involvement of ribosomal protein L6 in assembly of functional 50S ribosomal subunit in *Escherichia coli* cells. *Biochemical and Biophysical Research Communications*. 2016; 473: 237–242.
- [72] Zhang J, Ma Q, Han Y, Wen H, Zhang Z, Hao Y, *et al.* Down-regulated RPL6 inhibits lung cancer cell proliferation and migration and promotes cell apoptosis by regulating the AKT signaling pathway. *Journal of Thoracic Disease*. 2022; 14: 507–514.
- [73] Xia Y, Zhang X, Sun D, Gao Y, Zhang X, Wang L, *et al.* Effects of water-soluble components of atmospheric particulates from rare earth mining areas in China on lung cancer cell cycle. *Particle and Fibre Toxicology*. 2021; 18: 27.
- [74] Gou Y, Shi Y, Zhang Y, Nie Y, Wang J, Song J, *et al.* Ribosomal protein L6 promotes growth and cell cycle progression through upregulating cyclin E in gastric cancer cells. *Biochemical and Biophysical Research Communications*. 2010; 393: 788–793.
- [75] Wei J, Kishton RJ, Angel M, Conn CS, Dalla-Venezia N, Mar-

- cel V, *et al.* Ribosomal Proteins Regulate MHC Class I Peptide Generation for Immunosurveillance. *Molecular Cell*. 2019; 73: 1162–1173.e5.
- [76] Yoshihama M, Uechi T, Asakawa S, Kawasaki K, Kato S, Higa S, *et al.* The human ribosomal protein genes: sequencing and comparative analysis of 73 genes. *Genome Research*. 2002; 12: 379–390.
- [77] Yang CZ, Zang WC, Ji YP, Li TT, Yang YF, Zheng XF. Ribosomal protein L6 (RPL6) is recruited to DNA damage sites in a poly (ADP-ribose) polymerase-dependent manner and regulates the DNA damage response. *Journal of Biological Chemistry*. 2019; 294: 2827–2838.
- [78] Rashid M, Shah SG, Natu A, Verma T, Rauniyar S, Gera PB, *et al.* RPS13, a potential universal reference gene for normalisation of gene expression in multiple human normal and cancer tissue samples. *Molecular Biology Reports*. 2021; 48: 7967–7974.
- [79] Jackson SP, Bartek J. The DNA-damage response in human biology and disease. *Nature*. 2009; 461: 1071–1078.
- [80] Ciccia A, Elledge SJ. The DNA damage response: making it safe to play with knives. *Molecular Cell*. 2010; 40: 179–204.
- [81] Hopkins JL, Lan L, Zou L. DNA repair defects in cancer and therapeutic opportunities. *Genes and Development*. 2022; 36: 278–293.
- [82] Mortezaee K, Salehi E, Mirtavoos-Mahyari H, Motevaseli E, Najafi M, Farhood B, *et al.* Mechanisms of apoptosis modulation by curcumin: Implications for cancer therapy. *Journal of Cellular Physiology*. 2019; 234: 12537–12550.
- [83] Sapio RT, Nezdyur AN, Krevetski M, Anikin L, Manna VJ, Minkovsky N, *et al.* Inhibition of post-transcriptional steps in ribosome biogenesis confers cytoprotection against chemotherapeutic agents in a p53-dependent manner. *Scientific Reports*. 2017; 7: 9041.
- [84] Ko CY, Lin CH, Chuang JY, Chang WC, Hsu TI. MDM2 Downregulates Deacetylated Nucleolin Through Ubiquitination to Promote Glioma Stem-Like Cell Enrichment for Chemotherapeutic Resistance. *Molecular Neurobiology*. 2018; 55: 3211–3223.
- [85] Amar-Schwartz A, Ben Hur V, Jbara A, Cohen Y, Barnabas GD, Arbib E, *et al.* S6K1 phosphorylates Cdk1 and MSH6 to regulate DNA repair. *eLife*. 2022; 11: e79128.
- [86] André F, Michiels S, Dessen P, Scott V, Suci V, Uzan C, *et al.* Exonic expression profiling of breast cancer and benign lesions: a retrospective analysis. *The Lancet Oncology*. 2009; 10: 381–390.
- [87] Ladd JJ, Chao T, Johnson MM, Qiu J, Chin A, Israel R, *et al.* Autoantibody signatures involving glycolysis and spliceosome proteins precede a diagnosis of breast cancer among postmenopausal women. *Cancer Research*. 2013; 73: 1502–1513.
- [88] Yin X, Chen Y, Ruze R, Xu R, Song J, Wang C, *et al.* The evolving view of thermogenic fat and its implications in cancer and metabolic diseases. *Signal Transduction and Targeted Therapy*. 2022; 7: 324.
- [89] Anurag M, Jaehnig EJ, Krug K, Lei JT, Bergstrom EJ, Kim BJ, *et al.* Proteogenomic Markers of Chemotherapy Resistance and Response in Triple-Negative Breast Cancer. *Cancer Discovery*. 2022; 12: 2586–2605.
- [90] Qiang L, Wang L, Kon N, Zhao W, Lee S, Zhang Y, *et al.* Brown remodeling of white adipose tissue by SirT1-dependent deacetylation of Ppar γ . *Cell*. 2012; 150: 620–632.
- [91] Varghese E, Samuel SM, Líšková A, Samec M, Kubatka P, Büselberg D. Targeting Glucose Metabolism to Overcome Resistance to Anticancer Chemotherapy in Breast Cancer. *Cancers*. 2020; 12: 2252.
- [92] Gao X, Zhou S, Qin Z, Li D, Zhu Y, Ma D. Upregulation of HMGB1 in tumor-associated macrophages induced by tumor cell-derived lactate further promotes colorectal cancer progression. *Journal of Translational Medicine*. 2023; 21: 53.
- [93] Lee KM, Giltane JM, Balko JM, Schwarz LJ, Guerrero-Zotano AL, Hutchinson KE, *et al.* MYC and MCL1 cooperatively promote chemotherapy-resistant breast cancer stem cells via regulation of mitochondrial oxidative phosphorylation. *Cell Metabolism*. 2017; 26: 633–647.e7.
- [94] Mathieu J, Zhang Z, Zhou W, Wang AJ, Heddleston JM, Pinna CMA, *et al.* HIF induces human embryonic stem cell markers in cancer cells. *Cancer Research*. 2011; 71: 4640–4652.
- [95] Uniacke J, Perera JK, Lachance G, Francisco CB, Lee S. Cancer cells exploit eIF4E2-directed synthesis of hypoxia response proteins to drive tumor progression. *Cancer Research*. 2014; 74: 1379–1389.
- [96] Evans KW, Yuca E, Scott SS, Zhao M, Paez Arango N, Cruz Pico CX, *et al.* Oxidative phosphorylation is a metabolic vulnerability in chemotherapy-resistant triple-negative breast cancer. *Cancer Research*. 2021; 81: 5572–5581.
- [97] West CM, Davidson SE, Elyan SA, Valentine H, Roberts SA, Swindell R, *et al.* Lymphocyte radiosensitivity is a significant prognostic factor for morbidity in carcinoma of the cervix. *International Journal of Radiation Oncology Biology Physics*. 2001; 51: 10–15.